Cell

Global Regulation of H2A.Z Localization by the INO80 Chromatin-Remodeling Enzyme Is Essential for Genome Integrity

Manolis Papamichos-Chronakis,[1,3] Shinya Watanabe,[1] Oliver J. Rando,[2] and Craig L. Peterson[1,*]
[1]Program in Molecular Medicine
[2]Department of Biochemistry and Molecular Pharmacology
University of Massachusetts Medical School, Worcester, MA 01655, USA
[3]Present Address: Institut Curie, UMR218 CNRS, 26 rue d'Ulm, 75248 Paris Cedex 5, France, INSERM, ATIP-Avenir team, 75248 Paris Cedex 5, France
*Correspondence: craig.peterson@umassmed.edu
DOI 10.1016/j.cell.2010.12.021

SUMMARY

INO80 is an evolutionarily conserved, ATP-dependent chromatin-remodeling enzyme that plays roles in transcription, DNA repair, and replication. Here, we show that yeast INO80 facilitates these diverse processes at least in part by controlling genome-wide distribution of the histone variant H2A.Z. In the absence of INO80, H2A.Z nucleosomes are mislocalized, and H2A.Z levels at promoters show reduced responsiveness to transcriptional changes, suggesting that INO80 controls H2A.Z dynamics. Additionally, we demonstrate that INO80 has a histone-exchange activity in which the enzyme can replace nucleosomal H2A.Z/H2B with free H2A/H2B dimers. Genetic interactions between *ino80* and *htz1* support a model in which INO80 catalyzes the removal of unacetylated H2A.Z from chromatin as a mechanism to promote genome stability.

INTRODUCTION

DNA damage and aberrant chromosome replication can jeopardize genome integrity with serious effects to an organism's health and survival. Several mechanisms have evolved in eukaryotic cells to cope with damaged DNA and to promote proper duplication of the genome. During recent years, it has become apparent that chromatin structure plays an essential role in maintaining genomic integrity (Groth et al., 2007; Peterson and Cote, 2004). Specialized chromatin structures are formed during the DNA damage response or within S phase, promoting DNA repair and stabilizing replication forks. However, our understanding of how chromatin contributes to genome stability remains limited.

In addition to posttranslational modifications of histones, the building blocks of chromatin, incorporation of variant histones within chromatin regions provides an additional regulatory mechanism (Talbert and Henikoff, 2010). Histone variants such as H3.3 and H2A.Z are expressed throughout the cell cycle, and they can be incorporated into chromatin in the absence of DNA replication. Incorporation of the H2A-like H2A.Z into nucleosomal arrays alters their biophysical properties (Fan et al., 2002, 2004), potentially creating distinct chromatin structures that may regulate diverse metabolic processes. H2A.Z is highly conserved from yeast to human, and likewise the H2A.Z variant is enriched within nucleosomes at the proximal promoter regions of euchromatic genes of all eukaryotes (Mavrich et al., 2008; Raisner et al., 2005; Zhang et al., 2005). H2A.Z is also highly dynamic, being lost from promoters upon transcriptional activation at a rate that exceeds that of the core H3/H4 tetramer (Hardy et al., 2009; Zhang et al., 2005).

The SWI2/SNF2 family of ATP-dependent chromatin-remodeling enzymes use the energy of ATP hydrolysis to alter histone-DNA interactions, leading to movements of nucleosomes in *cis* (sliding), loss of some or all histones, or the exchange of H2A/H2B dimers (Clapier and Cairns, 2009). The Ino80 and Swr1 ATPases belong to the INO80 subfamily of the SWI2/SNF2 group of remodeling enzymes (Morrison and Shen, 2009). Both Swr1 and Ino80 are subunits of highly conserved, multisubunit complexes, SWR-C and INO80, that share several common subunits (e.g., Rvb1,2) (Kobor et al., 2004; Krogan et al., 2003; Mizuguchi et al., 2004; Shen et al., 2000). INO80 can catalyze nucleosome sliding in *cis* (Shen et al., 2000), whereas SWR-C, or its metazoan ortholog SRCAP (Kobor et al., 2004; Krogan et al., 2003; Mizuguchi et al., 2004; Ruhl et al., 2006), directs incorporation of H2A.Z into nucleosomes by a dimer-exchange reaction (Mizuguchi et al., 2004). In addition to a role in transcription, genetic studies indicate that INO80 regulates the DNA damage checkpoint response (Morrison et al., 2007; Papamichos-Chronakis et al., 2006) and stabilizes stalled replication forks (Papamichos-Chronakis and Peterson, 2008). Even though the importance of INO80 in genome stability is apparent, it is still unclear how INO80 contributes to these processes.

Here, we investigate the molecular mechanism of INO80 function in budding yeast. We present evidence indicating that INO80 regulates the genome-wide distribution of H2A.Z and that it promotes the eviction of H2A.Z from promoters during transcriptional induction. We also demonstrate that purified INO80

complex can incorporate H2A into an H2A.Z nucleosome in vitro, indicating that it has a histone-exchange activity that replaces nucleosomal H2A.Z/H2B with free H2A/H2B dimers. Notably, glutamine substitutions of the four N-terminal acetylatable lysine residues of H2A.Z alleviate the sensitivity of *ino80* mutants to both replication stress and DNA damage-inducing agents. Our data suggest that removal and replacement of unacetylated H2A.Z from chromatin by INO80 is an essential mechanism for maintaining genome integrity.

RESULTS

Aberrant Genome-wide Localization of H2A.Z in the Absence of INO80

Previously, we reported that a partial deletion of the *INO80* gene (*ino80Δ300*) led to increased levels of H2A.Z within chromatin that surrounded a single, unrepaired DNA double-strand break (DSB) (Papamichos-Chronakis et al., 2006). When H2A.Z distribution was analyzed by chromatin immunoprecipitation in a strain harboring a complete deletion of INO80 (*ino80Δ*), altered levels of H2A.Z were detected at many genomic locations even in the absence of a DSB (data not shown). In order to understand how H2A.Z localization may be altered upon inactivation of the INO80 complex, we analyzed the distribution of H2A.Z across 4% of the genome (chromosome III and 230 additional promoter regions) at single nucleosome resolution using a combination of mononucleosome-resolution ChIP with dense tiling microarrays (ChIP-chip). Briefly, cells from wild-type (WT) and *ino80Δ* strains were arrested in the G1 phase of the cell cycle, cells were fixed with formaldehyde, cross-linked chromatin was digested to mononucleosomes, and chromatin immunoprecipitation was conducted with a polyclonal antibody directed against H2A.Z. Total and immunoprecipitated DNA from the two strains were subsequently amplified, labeled with Cy3 and Cy5, and hybridized to a custom, high-resolution tiling microarray (Liu et al., 2005; Yuan et al., 2005).

In agreement with published results, the mononucleosomal H2A.Z map produced from the WT cells confirmed the distinct enrichment pattern of H2A.Z (Figures 1C and 1F). H2A.Z enrichment spanned a wide dynamic range, with the 2.5% most-enriched nucleosomes exhibiting 16-fold enrichment of H2A.Z relative to the 2.5% most H2A.Z-depleted nucleosomes (Figure 1A). However, the dynamic range of nucleosomal H2A.Z levels in the *ino80Δ* mutant was significantly compressed, with 95% of nucleosomes captured within a 6-fold dynamic range (Figure 1A). This is visualized by plotting nucleosome enrichments for H2A.Z in the *ino80Δ* cells against those of the WT cells, showing that the slope of WT versus *ino80Δ* enrichments is well below one (y = 0.547x) (Figure 1B). Because of standard microarray normalization, these data are equally consistent with global overincorporation of H2A.Z, global underincorporation, or mixed gain and loss at specific loci. However, equal levels of bulk, chromatin-associated H2A.Z were detected in the WT and *ino80Δ* strains (Figure 1D). These results indicate that INO80 does not impact the total amount of H2A.Z that is incorporated into chromatin, but rather there is an extensive reorganization of nucleosomal H2A.Z across the genome in the absence of Ino80. This can be seen at many loci as spurious incorporation of H2A.Z in the *ino80Δ* mutant strain, together with a drop in H2A.Z levels at H2A.Z-rich domains (Figure 1C and Figure S1 available online).

To gain further insight into the regulation of H2A.Z localization by the INO80 complex, we focused on RNAPII-transcribed genes. The typical open reading frame is characterized by high levels of H2A.Z at the first nucleosome (+1) at the transcription start site (TSS), with variable H2A.Z at the upstream (−1) nucleosome and low levels of H2A.Z downstream of the +1 nucleosome (Albert et al., 2007; Raisner et al., 2005; Zhang et al., 2005). As shown in Figure 1E, H2A.Z mislocalization was especially pronounced at promoter nucleosomes (y = 0.487x). Interestingly, the decrease of H2A.Z at the +1 nucleosome was associated with concomitant gain of H2A.Z at nucleosomes inside the coding sequences [mid- and 3′ coding sequence (CDS)], (Figure 1F). Together, these data demonstrate that H2A.Z becomes globally mislocalized in the *ino80Δ* mutant, and they support a role for the INO80 complex in regulating proper genome-wide H2A.Z localization.

The INO80 Complex Promotes Transcription-Associated H2A.Z Dynamics

In budding yeast, H2A.Z occupancy negatively correlates with transcription rates, with H2A.Z being highly enriched in most gene promoters but depleted upstream of very highly transcribed genes (Zhang et al., 2005). As an initial test to investigate whether INO80 plays a role in this process, a mononucleosomal ChIP-chip assay for H2A.Z was conducted in G1- and G2/M-arrested WT and *ino80Δ* cells. Scatter plot analysis of H2A.Z nucleosome occupancy demonstrated that H2A.Z genomic occupancy is altered between the two cell-cycle phases in the WT strain (y = 0.635x; Figure 2A). However, in the *ino80Δ* mutant, the H2A.Z nucleosomal pattern remains largely unchanged, consistent with INO80 regulating the dynamics of H2A.Z-containing nucleosomes (y = 0.953x; Figure 2B).

Expression of *KAR4* is highly induced when cells are arrested in G1 by mating pheromone, and it is repressed in G2 phase (Kurihara et al., 1996). As shown in the heat maps of the *KAR4* locus in the WT strain (Figure 2C, left), H2A.Z is enriched at the repressed *KAR4* promoter in G2/M and becomes, as expected, depleted during transcriptional activation in G1 cells. As expected, the enrichment of H2A.Z at other, non-cell-cycle-regulated genes remains unchanged between G1 and G2/M samples (Figure S2C). In contrast, H2A.Z levels in the *ino80Δ* mutant remain high and similar to the repressed level in both G1 and G2/M phases (Figure 2C, right). Notably, induction of *KAR4* expression is not affected by inactivation of Ino80 (Figure S2A), and thus transcription levels do not explain the altered H2A.Z dynamics. These results also indicate that the failure to deplete H2A.Z during transcriptional induction has little effect on *KAR4* expression. These results suggest that INO80 controls either the eviction of the H2A.Z/H2B dimers or the loss of H2A.Z-containing nucleosomes that occurs during transcriptional induction.

INO80 Regulates Transcription-Dependent H2A.Z Eviction

To investigate how INO80 controls H2A.Z dynamics, we used nucleosome-scanning analysis at the *KAR4* locus. Forty-five overlapping primer pairs were used to monitor the translational

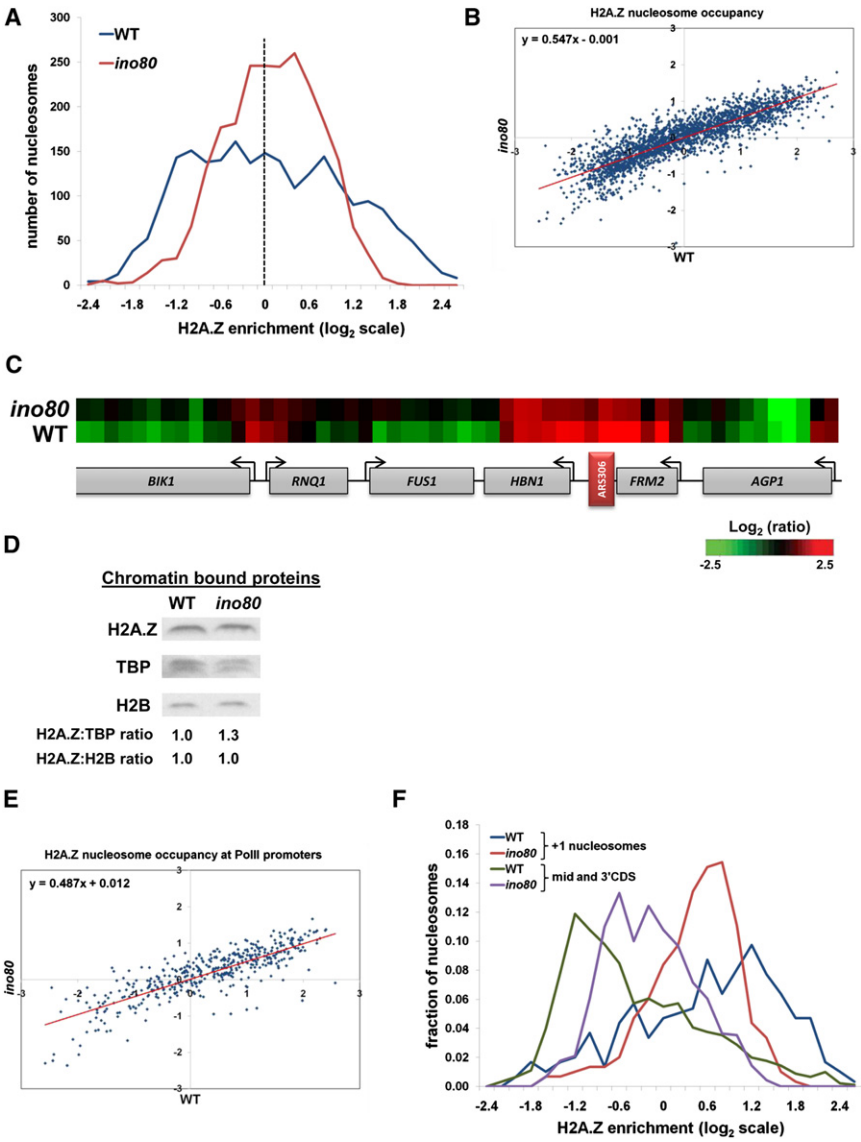

Figure 1. Global Alterations in the H2A.Z Nucleosomal Incorporation upon Disruption of the INO80 Complex

(A–C) Increased misincorporation of H2A.Z and compression of the H2A.Z-enrichment range in the absence of *INO80* as measured by mononucleosomal ChIP-chip analysis. (A) Distribution of the $\log_2$ median ratios of H2A.Z enrichment in WT and *ino80* nucleosome populations. Value 0 on the x axis reflects the average H2A.Z enrichment in each strain. (B) Scatter plot analysis comparing H2A.Z enrichment in WT versus *ino80* mutant. Blue dots represent H2A.Z nucleosomes. The trendline equation indicates the global change of the distribution of H2A.Z in the *ino80* strain compared to WT. (C) Heatmap from a mononucleosomal ChIP-chip experiment for H2A.Z conducted in WT and *ino80* cells. Each box represents 140 nucleotides. Squares in the same column represent the same nucleosomes. Green signal indicates H2A.Z enrichment below average and red signal indicates positive enrichment. Black indicates average enrichment. Scheme represents the respective scanned region of chromosome III.

(D) Equal levels of chromatin-bound H2A.Z in WT and *ino80* strains. Chromatin fractions were isolated from WT and *ino80* cells and immunoblot analysis was performed for the indicated proteins. Similar results were found when nucleosomal histones were released from the chromatin pellet by MNase digestion prior to the SDS-PAGE analysis (data not shown).

(E and F) Pronounced mislocalization of H2A.Z at RNA PolII genes. (E) Scatter plot analysis comparing H2A.Z enrichment at promoter nucleosomes in the indicated strains. Analysis conducted as in (B). (F) Distribution analysis of H2A.Z enrichment at the first nucleosome downstream of TSS (+1 nucleosomes) and in the coding sequence (mid- and 3′ CDS) in WT and *ino80* strains. Analysis conducted as in (A).

See also Figure S1.

position and dynamics of H2A.Z nucleosomes at the *KAR4* promoter in the presence or absence of *INO80*. When samples were analyzed from G2/M-arrested WT or *ino80* cells, this analysis yielded four peaks, indicating four positioned nucleosomes flank the *KAR4* promoter in the repressed state (Figure 2D). Notably, the positioning of these promoter proximal nucleosomes was identical in the presence or absence of Ino80 (Figure 2D). Strikingly, *KAR4* promoter sequences were also severely depleted from mononucleosome samples of both G1-arrested WT and *ino80* cells, indicating that nucleosomes are depleted when *KAR4* is expressed (Figures 2D and 2E).

To measure H2A.Z occupancy at *KAR4* promoter nucleosomes, we conducted chromatin immunoprecipitation of H2A.Z. In the repressed state (G2/M), H2A.Z is enriched at each of the four promoter nucleosomes, with the highest levels seen for nucleosome +1 (Figure 2F). At this promoter, similar levels are observed in the *ino80Δ* mutant, as expected from Figure 2C. Upon activation of *KAR4* (G1 cells), the amount of H2A.Z per nucleosome is lower at several *KAR4* nucleosomes in the WT strain, indicating that H2A.Z is evicted (Figure 2G and Figure S2B). In contrast, the amount of H2A.Z per nucleosome does not decrease in the *ino80Δ* mutant, with levels remaining at the repressed, G2/M level or even higher (Figure 2G and Figure S2B). Taken together, these results suggest two independent and complementary pathways for H2A.Z eviction—the first pathway is driven by complete nucleosome loss, and the second, H2A.Z-specific eviction, requires INO80.

INO80 Exchanges Nucleosomal H2A.Z/H2B with Free H2A/H2B Dimers In Vitro

These data indicate that INO80 regulates the genome-wide localization of H2A.Z as well as the eviction of H2A.Z during

transcriptional induction. One simple possibility is that INO80 might preferentially slide H2A.Z nucleosomes or evict H2A.Z octamers during transcriptional induction. However, INO80 shows no detectable octamer eviction activity with either H2A or H2A.Z mononucleosomes, and we find that INO80 mobilizes H2A or H2A.Z nucleosomes with equal efficiency (Figures S3A and S3B). Since Ino80 and Swr1 belong to the same subfamily of Snf2-like ATPases, we tested whether Ino80 might catalyze an ATP-dependent H2A.Z/H2B dimer-exchange event that removes H2A.Z and incorporates H2A.

Histone-exchange assays were performed with mononucleosomes reconstituted with recombinant yeast histones. Initially, mononucleosomes were assembled with H2A/H2B dimers, and these substrates were incubated with remodeling enzyme and free HA-tagged H2A.Z/H2B dimers. Following incubation, the reactions were electrophoresed on native PAGE to separate bona fide mononucleosome products from free histones or other types of nucleosomal products. Histone exchange was evaluated by western blotting, probing for loss of H2A and incorporation of HA-tagged H2A.Z into the mononucleosome (Figure 3A). In all experiments, mononucleosome integrity was analyzed by both western analysis of histone H2B and by visualizing DNA with ethidium bromide (Figure 3 and data not shown). As expected, the SWR-C complex showed robust, ATP-dependent incorporation of HA-H2A.Z and significant loss of H2A. In contrast, and consistent with previous studies, Ino80 showed little activity in this H2A.Z incorporation assay (Figure 3B and Figure S3E). Importantly, these same preparations of Ino80 showed robust ATPase and nucleosomal sliding activities (Figures S3B–S3D).

Next, mononucleosomes were assembled with H2A.Z/H2B dimers and incubated with remodeling enzyme and FLAG-tagged H2A/H2B dimers. Strikingly, Ino80 catalyzed ATP-dependent incorporation of FLAG-H2A into a mononucleosome product, whereas SWR-C, SWI/SNF, and RSC were inactive on this substrate (Figure 3C and data not shown). The INO80-dependent incorporation of FLAG-H2A was concentration dependent and increased with time of incubation (Figure 3D and data not shown), and titration of the mononucleosome substrate indicates that efficient exchange activity for 5 nM INO80 requires > 50 nM nucleosomes (data not shown). Strikingly, INO80 action catalyzed removal of 35% of the H2A.Z from the initial mononucleosome substrate, while the levels of H2B remained constant (Figure 3E). Notably, INO80 does not exhibit promiscuous dimer eviction activity, as INO80 does not catalyze H2A eviction from an H2A-containing mononucleosome (Figure S3E). Thus, these data indicate that INO80 catalyzes a dimer-exchange reaction in which nucleosomal H2A.Z/H2B is replaced with an H2A/H2B dimer.

Previous analyses of ATP-dependent dimer-exchange activities have used biotinylated chromatin substrates immobilized on streptavidin magnetic beads (Mizuguchi et al., 2004). In these assays, the immobilized substrate is incubated with remodeling enzyme and free histones, and exchange events are monitored by western blot following magnetic bead capture of the chromatin substrate. We performed this strategy with biotinylated mononucleosomes reconstituted with H2A.Z/H2B dimers, and we found that Ino80 catalyzed FLAG-H2A incorporation in this assay as well (Figure 3F). Furthermore, no detectable incorporation of FLAG-H2A was observed when INO80 was incubated with a mononucleosome reconstituted with an H2A/H2B dimer (Figure 3G). Together, both types of assays indicate that INO80 can specifically replace nucleosomal H2A.Z with H2A.

Decreased H2A.Z Expression Rescues Replication Defects of an *ino80* Mutant

INO80 plays roles in many nuclear events, including gene transcription, DNA replication, DNA repair, and sister chromatid cohesion (Conaway and Conaway, 2009). One possibility is that INO80 regulates these diverse events by its action on H2A.Z and, consequently, the defects observed in an *ino80* mutant may be due to the mislocalization and aberrant chromatin dynamics of H2A.Z. One simple prediction of this model is that H2A.Z depletion might rescue the defects of an *ino80* mutant. Unfortunately, *htz1Δ ino80Δ* and *swr1Δ ino80Δ* double mutants are inviable, suggesting that H2A.Z and Ino80 may play additional, redundant role(s) in an essential function (Figure S4A and data not shown). To overcome this problem, we created isogenic WT and *ino80Δ* strains in which *HTZ1* is expressed from a chromosomal, truncated promoter at ~10% WT levels ($HTZ1^{CP}$) (Figure 4A). This reduced expression of *HTZ1* leads to a 4-fold decrease in bulk H2A.Z chromatin association, and a ~2-fold decrease at the positioned nucleosomes of the *KAR4* locus (Figure 4B and Figure S4B). The $HTZ1^{CP}$ allele fully complements the growth defect and thiobendazol sensitivity of an *htz1Δ* strain (data not shown), indicating that this level of H2A.Z is sufficient to perform its known functions.

Previously, we showed that *ino80* cells are incapable of completing DNA replication when exposed to replication stress conditions (Papamichos-Chronakis and Peterson, 2008). We investigated whether decreased expression of H2A.Z can rescue this replication defect. WT and *ino80Δ* cells that expressed either normal (*HTZ1*) or low levels of H2A.Z ($HTZ1^{CP}$) were arrested in G1 and then released into media containing 40 mM hydroxyurea (HU), and their progression through S phase was followed by fluorescence-activated cell sorting (FACS). Both *HTZ1* and $HTZ1^{CP}$ WT strains progressed normally through S phase (Figure 4C). As we showed previously, *ino80Δ* cells that express normal levels of H2A.Z are rapidly blocked in S phase (Figure 4C, left). Interestingly, lowering the expression of H2A.Z restored a normal rate of S phase progression in HU media in the absence of Ino80 (Figure 4C, right). In contrast, both the *ino80* and $HTZ1^{CP}$ *ino80* cells failed to grow in media lacking inositol (data not shown), indicating that lowered expression of *HTZ1* cannot support transcription of the *INO1* gene in the absence of *INO80*. Thus, these results indicate a close functional relationship between INO80 and H2A.Z and suggest that aberrant H2A.Z incorporation may have a negative impact on DNA replication fork stability.

Functional Interactions between INO80 Complex and H2A.Z Acetylation

The N-terminal domain of yeast H2A.Z is acetylated in vitro at lysines 3, 8, 10, and 14 by the NuA4 HAT complex (Babiarz et al., 2006; Keogh et al., 2006; Millar et al., 2006), and

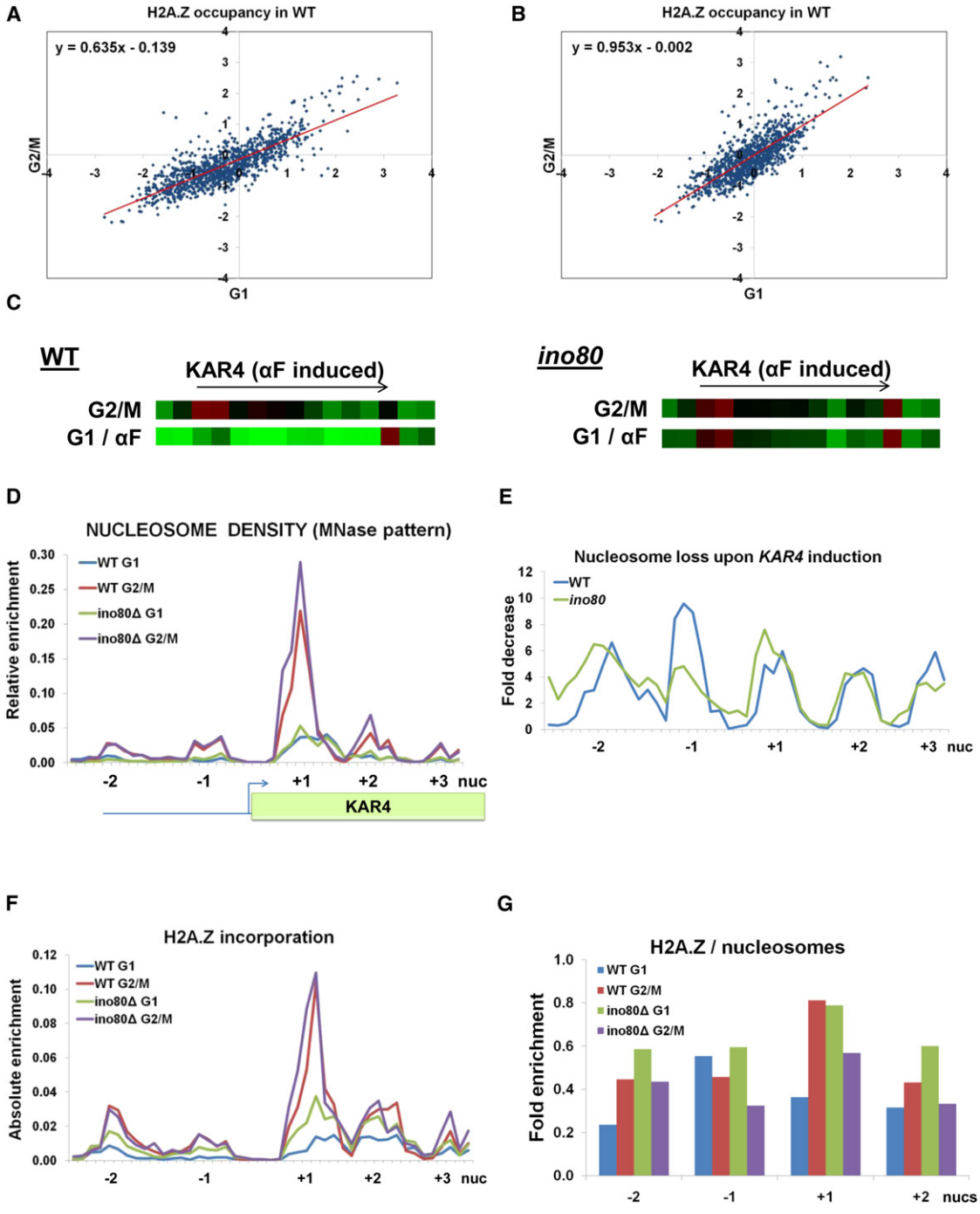

Figure 2. H2A.Z Is Not Lost from Nucleosomes in the Absence of *INO80*

(A and B) Scatter plot analyses comparing H2A.Z enrichment in G2/M- versus G1-arrested WT (A) and *ino80* mutant (B) cells.

(C) Indicative heatmaps of H2A.Z nucleosomal occupancy at the *KAR4* locus under repressed (G2/M) and activated (G1) conditions in the indicated strains.

(D and E) Nucleosome positioning and nucleosome loss at the *KAR4* promoter. (D) Representative graph demonstrating nucleosome positioning in WT and *ino80* cells at the indicated conditions as measured by amplification of genomic mononucleosomal DNA by qPCR. Values reflect the ratio of the amplified tested DNA over the total DNA purified from mononucleosomes. Scheme represents the promoter and coding region of *KAR4*. Numbers of the nucleosomes are relative to the TSS. (E) Nucleosome loss was measured from (D) as the fold decrease of the DNA amplified in repressed overinduced conditions after correction of the ratios of amplification achieved with total MNased DNA.

(F and G) H2A.Z is not evicted from the *KAR4* promoter during transcriptional induction in the *ino80* strain. (F) Mononucleosomal-ChIP assay for H2A.Z was conducted in the WT and *ino80* strains in the indicated conditions. Values reflect the average absolute amplification of the tested DNA from three independent

acetylation occurs at promoter nucleosomes in vivo after incorporation of H2A.Z into chromatin by SWR-C (Keogh et al., 2006). Given that H2A.Z was mislocalized in the absence of Ino80, we tested whether H2A.Z acetylation levels might be altered in the *ino80Δ* mutant. Strikingly, H2A.Z-K14 acetylation levels were much lower in the *ino80Δ* strain compared to WT (Figure 5A).

We entertained the possibility that this defect in H2A.Z acetylation contributes to the genome instability phenotypes of the *ino80Δ* mutant. However, a strain that harbors a derivative of H2A.Z that cannot be acetylated, H2A.Z-K3,8,10,14R, does not show sensitivity to DNA damage or replication stress agents (Millar et al., 2006), indicating that the lack of H2A.Z acetylation is insufficient to cause genome instability phenotypes. Interestingly, H2A.Z-K3,8,10,14R shows synthetic sensitivity to replication stress and DNA damage agents when expressed in an *ino80Δ* strain (Figure 5B). These results reveal a role for Htz1 acetylation in DDR and replication stress survival and suggest a functional connection between H2A.Z acetylation and INO80.

HDA1 encodes a histone deacetylase that regulates H2A.Z acetylation (Lin et al., 2008). As shown in Figure 5A, inactivation of Hda1 led to a large increase in H2A.Z-K14 acetylation in both the WT and *ino80* strains. These data support a simple model in which H2A.Z can be acetylated in the absence of INO80, but it is deacetylated by Hda1, possibly due to its mislocalization.

This data raise the interesting possibility that the accumulation of deacetylated H2A.Z in the *ino80* mutant might be detrimental to genome stability. Deletion of *HDA1* renders cells sensitive to DNA damage-inducing agents like methylmethanesulfonate (MMS) and zeocin but not to replication stress induced by hydroxyurea (Begley et al., 2002 and Figure S5). In our initial studies, we found that an *ino80Δ hda1Δ* double mutant has a severe slow-growth phenotype that made growth assays problematic. To circumvent this issue, we monitored the phenotype of an *arp8Δ hda1Δ* double mutant that did not show this synthetic phenotype. The Arp8 subunit is essential for the chromatin-remodeling activities of INO80, and an *arp8Δ* mutant shows sensitivity to replication stress (HU treatment) and DNA damaging agents (zeocin). Strikingly, deletion of *HDA1* suppresses the HU sensitivity of an *arp8Δ* mutant (Figure 5C). These results suggest that the replication defects caused by inactivation of the INO80 complex can be rescued by removing the Hda1 HDAC.

The H2A.Z-K(3,8,10,14)Q Acetylation Mimic Suppresses Genomic Instability Caused by Disruption of the INO80 Complex

To further test whether constitutive H2A.Z acetylation can alleviate *ino80Δ* phenotypes, we created a putative H2A.Z acetyl mimic (*HTZ1 K3,8,10,14Q*). Initially, we tested whether expression of H2A.Z-K3,8,10,14Q could rescue the replication defects of an *arp8* mutant during replication stress conditions. WT and *arp8* cells that express either H2A.Z or H2A.Z-K3,8,10,14Q were arrested in G1 and subsequently released into 40 mM HU, and their progression through S phase was followed by FACS. As shown in Figure 6A, WT cells progressed through S phase and completed DNA replication in approximately 100 min. In contrast, the *arp8* cells proceeded through S phase slowly, unable to fully replicate their genome even after almost 6 hr in HU. However, expression of the H2A.Z panacetyl mimic in the *arp8* strain enabled cells to duplicate their genome, albeit slowly (Figure 6A). In addition, expression of the H2A.Z panacetyl mimic appears to alleviate the fork collapse phenotype of an *arp8* mutant, as WT levels of DNA polα are recovered at a stalled replication fork in the absence of Arp8 (Figure S6A). Expression of H2A.Z-K3,8,10,14Q also alleviated the growth sensitivity of *arp8*, *arp5*, and *ino80* mutants to HU, as well as to the DNA damage-inducing agents MMS and zeocin (Figure 6B). Importantly, the *htz1-4KQ* strain has no apparent phenotype in the presence of INO80 (Figure S6B). In contrast, expression of H2A.Z-K3,8,10,14Q did not alleviate the MMS or HU sensitivity of an *mre11Δ* mutant (Figure S6C), indicating that suppression is specific to mutations that disrupt the INO80 complex. Interestingly, expression of H2A.Z-K3,8,10,14Q did not suppress the inositol auxotrophy of an *arp8* mutant, and *ARP8*-dependent transcription of the *INO1* gene was not alleviated by H2A.Z-K3,8,10,14Q (Figures 6C and 6D). Importantly, suppression of *arp8Δ* genome stability phenotypes by the panacetyl mimic are eliminated after reintroduction of a WT copy of *HTZ1* (Figure 6E). These data indicate that H2A.Z-K3,8,10,14Q is a potent suppressor of the genomic instability phenotypes of strains that lack the INO80 complex.

One simple explanation for why the H2A.Z-K3,8,10,14Q might suppress *ino80* phenotypes posits that this H2A.Z derivative is not properly expressed or that it restores the WT chromatin distribution and dynamics of H2A.Z in the absence of Ino80. We find, however, that H2A.Z-K3,8,10,14Q is expressed and incorporated into chromatin at levels similar to WT as measured by ChIP and nucleosome-scanning assays (Figures S6B, S6D, and S6E). Moreover, mapping of H2A.Z-K3,8,10,14Q at *KAR4* nucleosomes demonstrated that both H2A.Z-K3,8,10,14Q and WT H2A.Z were incorporated in high amounts in the *arp8* mutant compared to the WT strain, and neither H2A.Z-K3,8,10,14Q nor H2A.Z were lost from *KAR4* promoter nucleosomes upon transcriptional induction in the absence of INO80 (Figures 6F and 6G). These results suggest that the activity of INO80 is not sensitive to the acetylation status of H2A.Z and that both WT and the H2A.Z-K3,8,10,14Q derivative require INO80 action for proper localization. Consistent with this view, the in vitro histone-exchange activity of INO80 is not affected by substitution of H2A.Z N-terminal lysines with either arginine or glutamine residues (Figure S6F and data not shown). Collectively, these results are consistent with a model in which the mislocalization of unacetylated H2A.Z in the absence of INO80 is detrimental to genome integrity but constitutive H2A.Z acetylation counteracts these inhibitory effects.

experiments. (G) Mononucleosomal-ChIP assay for H2A.Z was conducted in the WT and *ino80* strains in the indicated conditions. Values reflect the average enrichment of H2A.Z normalized to the respective input DNA from three independent experiments. Each bar represents the average enrichment of the tested DNA from six primer pairs inside the corresponding nucleosomal region.
See also Figure S2.

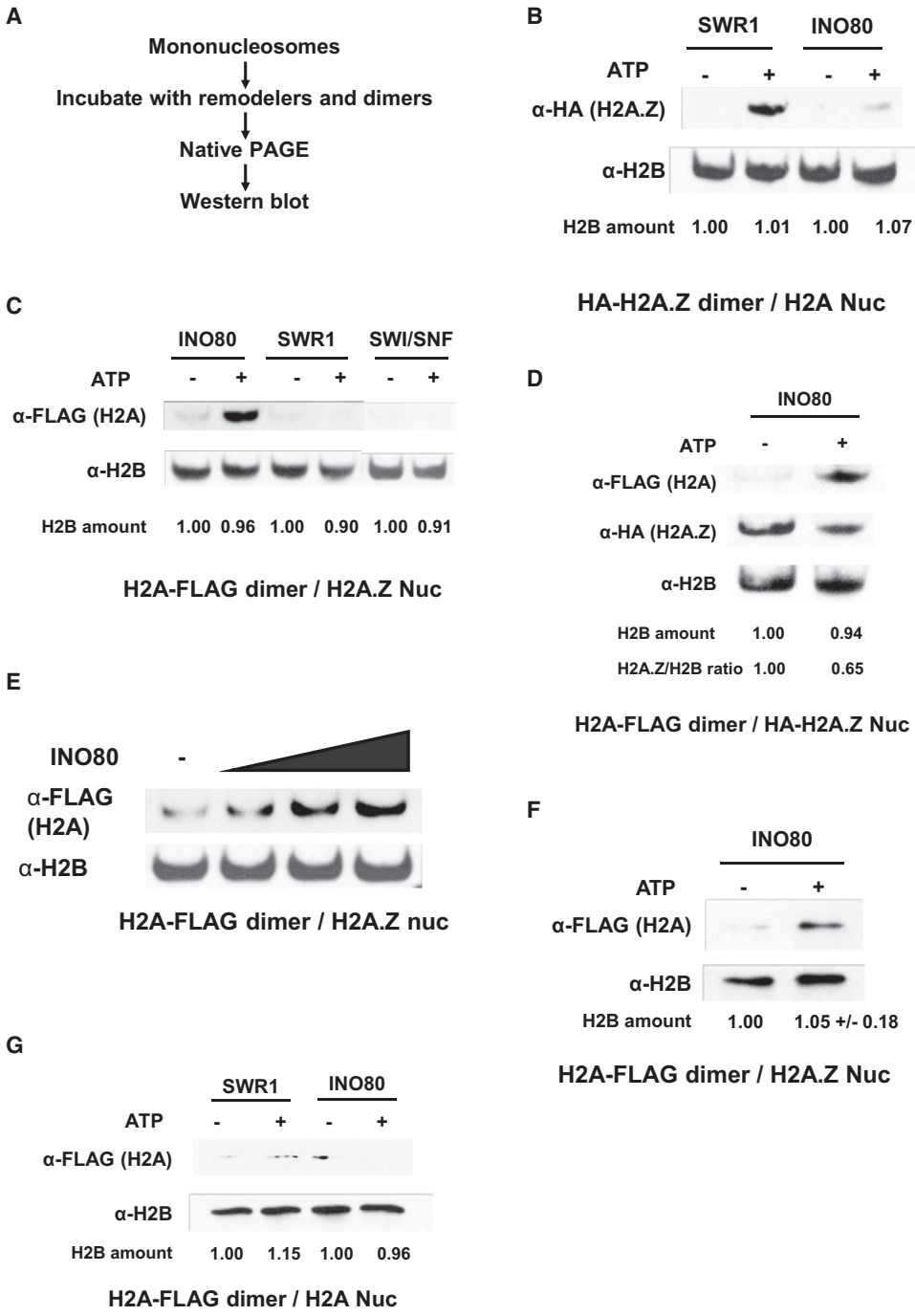

Figure 3. INO80 Has ATP-Dependent Histone-Exchange Activity

(A) Scheme of in vitro dimer-exchange assay with recombinant yeast mononucleosomes. Mononucleosomes were incubated with remodeling enzymes and free dimers. Incorporation of dimers into the nucleosomes was analyzed by native PAGE and western blotting.

(B) SWR-C incorporates H2A.Z/H2B dimers into H2A-containing nucleosomes. H2A-containing mononucleosomes (100 nM) were incubated with the indicated remodeling enzymes (5 nM) and free, HA-tagged H2A.Z/H2B dimers (50 nM) in the presence or absence of ATP.

(C) INO80 incorporates H2A/H2B dimers into H2A.Z-containing nucleosomes. H2A.Z-containing mononucleosomes (100 nM) were incubated with the indicated remodeling enzymes (5 nM) and free FLAG-tagged H2A/H2B dimers (50 nM) in the presence or absence of ATP.

(D) Concentration dependence of INO80 on H2A/H2B dimer incorporation activity. Increasing amounts (3, 6, and 12 nM) of INO80 was used as in (C).

(E) INO80 catalyzes a histone-exchange event. HA-tagged, H2A.Z-containing mononucleosomes (100 nM) were incubated with INO80 (5 nM) and free FLAG-tagged H2A/H2B dimers (50 nM) in the presence or absence of ATP.

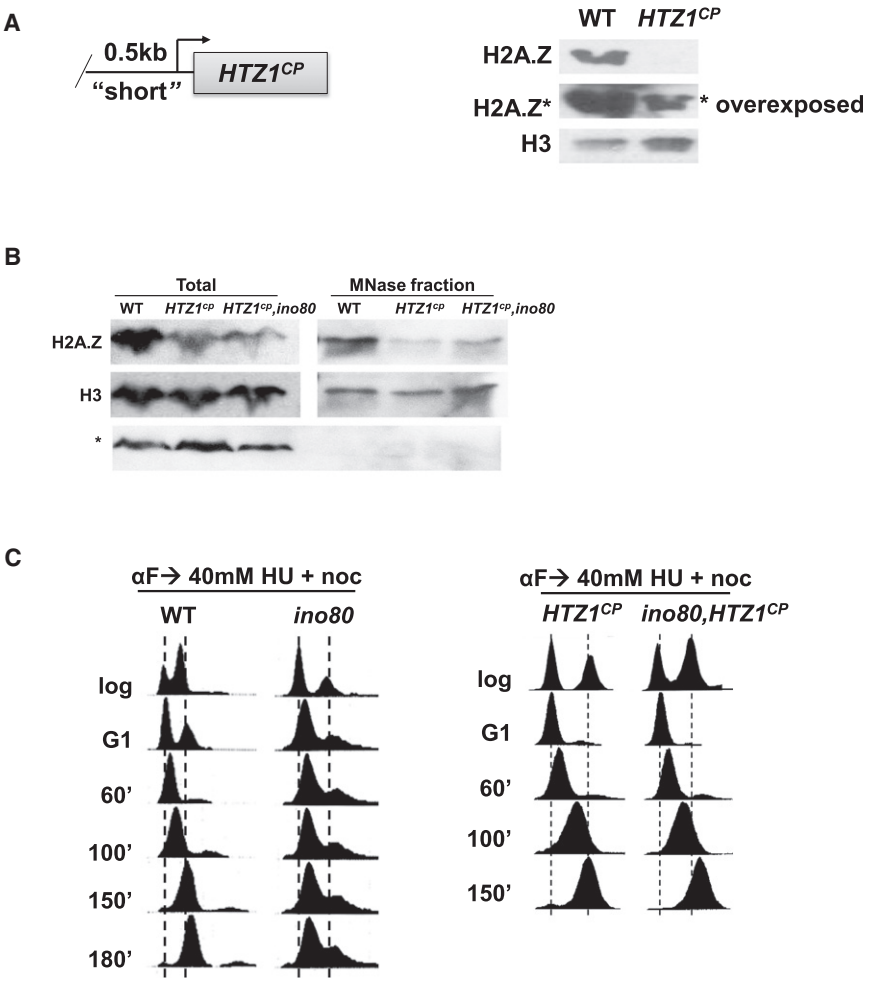

Figure 4. Reduced H2A.Z Expression Suppresses the Replication Defects of the *ino80* Mutant Strain

(A) Left: Schematic representation of the *HTZ1* locus carrying the truncated *HTZ1* promoter. Right: Reduced H2A.Zp levels from the crippled promoter. Acid-extracted proteins from logarithmically grown cells were separated by SDS-PAGE and immunoblot analysis was performed for H2A.Z. Equal gel loading was confirmed by western blotting against histone H3.

(B) Reduced incorporation of $HTZ1^{cp}$ in chromatin. Chromatin fractionation assay in WT, $HTZ1^{cp}$ and $HTZ1^{cp}$, and *ino80* strains and total and chromatin fraction of proteins were separated by SDS-PAGE and analyzed by immunoblotting for H2A.Z. The asterisk (*) indicates an apparent cytoplasmic protein that cross-reacts with the anti-H2A.Z antibody and serves as a fractionation control.

(C) Expression of $HTZ1^{cp}$ promotes replication during replication stress conditions in the absence of *INO80*. Cells from the indicated strains were synchronized in G1 phase with alpha factor (αF) and subsequently released into nocodazole-containing YPD media with 40 mM HU. Cell samples were collected at the indicated times and analyzed for DNA content by flow cytometry analysis.

See also Figure S4.

DISCUSSION

Whereas previous studies have focused on the key role of the yeast SWR-C- and mammalian SRCAP-remodeling enzymes in directing the ATP-dependent deposition of the H2A.Z histone variant, here we have shown that the related INO80 enzyme catalyzes the replacement of nucleosomal H2A.Z for H2A within coding regions and the eviction of H2A.Z during transcriptional activation. Interestingly, this role for INO80 appears essential for the maintenance of genome stability, as decreased expression of H2A.Z or expression of a H2A.Z panacetyl mimic alleviates the sensitivity of *ino80*, *arp5*, or *arp8* mutants to DNA-damaging or replication stress agents. Thus, our genetic interactions suggest that aberrant accumulation of unacetylated H2A.Z has a negative impact on DNA DSB repair and DNA replication fork stability.

ATP-Dependent Histone Exchange by the INO80 Subfamily of Enzymes

Although members of the SWI/SNF subfamily of remodeling enzymes are able to evict histone dimers or entire octamers from nucleosomal substrates, only members of the INO80 subfamily exhibit histone dimer deposition and/or exchange activity. Both the yeast SWR-C and mammalian SRCAP members can replace nucleosomal H2A with H2A.Z, and in this study we report that yeast INO80 can perform the opposite reaction, converting an H2A.Z mononucleosome into one that contains H2A. Why hasn't the dimer-exchange activity of INO80 been detected previously? We find that optimal dimer-exchange activity requires nucleosome concentrations >50 nM (S. W., unpublished data), whereas most previously published dimer-exchange assays have used much lower nucleosome concentrations (<10 nM; Mizuguchi et al., 2004). The Ino80 and Swr1 ATPases are the only members of the Snf2 family of ATPases that contain very large, ~300–500 amino acid insertions between Helicase/ATPase

(F) INO80 incorporates H2A/H2B dimers into H2A.Z-containing nucleosomes. Streptavidin bead-immobilized H2A.Z-containing, biotinylated mononucleosomes (100 nM) were incubated with INO80 (5 nM) and free FLAG-tagged H2A /H2B dimers (50 nM) in the presence or absence of ATP. After washing, incorporation of dimers into the nucleosomes was analyzed by SDS-PAGE and western blotting. H2B values reported in this experiment reflect the standard deviation from three independent experiments.

(G) INO80 does not incorporate H2A/H2B dimers into H2A-containing nucleosomes. H2A-containing biotinylated mononucleosomes (100 nM) were incubated with remodeling enzymes (5 nM) and free FLAG-tagged H2A/H2B dimers (50 nM) in the presence or absence of ATP.

See also Figure S3.

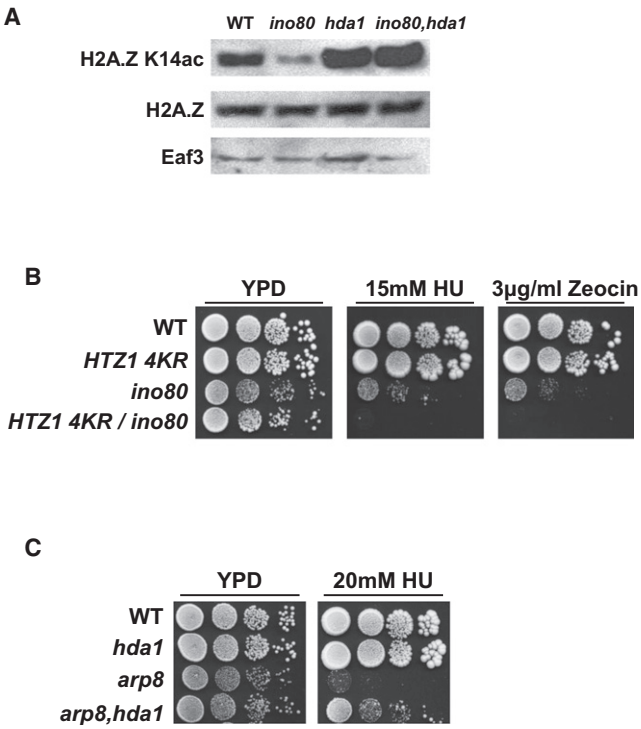

Figure 5. Functional Interactions between INO80 and H2A.Z Acetylation

(A) Decrease of H2A.Z-K14 acetylation in the *ino80* mutant is dependent on Hda1. Acid-extracted proteins from WT, *ino80*, *hda1*, and *ino80 hda1* double-mutant cells were separated by SDS-PAGE and assayed for total and K14 acetylated H2A.Z by western blotting. Equal gel loading was confirmed by immunoblot analysis against Eaf3.

(B) H2A.Z acetylation is essential for the viability of the *ino80* mutant cells in DNA damage and replication stress conditions. WT, *HTZ1-K(3,8,10,14)R* (*HTZ1 4KR*), *ino80*, and *ino80* mutant cells expressing the *HTZ1-K(3,8,10,14)R* derivative (*HTZ1 4KR,ino80*) were plated in 10-fold serial dilutions on YPD plates containing the indicated concentration of HU or zeocin to induce DNA replication stress or DNA DSBs, respectively. Pictures of the plates were taken after 2–5 days of incubation at 30°C.

(C) Deletion of *HDA1* suppresses the replication defects of the *arp8* strain during replication stress conditions. Log-phase cells from the indicated strains were plated in 10-fold serial dilutions on YPD plates containing 20 mM HU. Pictures of the plates were taken after 2–4 days of incubation at 30°C.

See also Figure S5.

motifs III and IV, and it seems likely that this insertion influences the outcome of the remodeling reaction (Clapier and Cairns, 2009). In addition, each enzyme has a unique complement of histone-binding subunits that may determine the specificity of the deposition reaction. For instance, the SWR-C contains the SWC2 subunit, key for H2A.Z recognition (Wu et al., 2005) as well as the Yaf9 subunit, which harbors a YEATS domain that binds H3/H4 (Wang et al., 2009). Furthermore, the SWR-C and INO80 complexes each harbor the Arp4 and Arp5 subunits that interact with H2A/H2B dimers (Shen et al., 2003), and previous mass spectrometry data indicate that both H2A and H2A.Z are associated with the purified INO80 complex even in the absence of DNA damage (Mizuguchi et al., 2004).

Regulation of H2A.Z Dynamics by the INO80 Complex

Why is H2A.Z mislocalized in the absence of INO80 and how is INO80 action targeted to create the WT pattern? The SWR-C enzyme is localized predominantly to the +1 and/or −1 nucleosomes proximal to many RNAPII promoters, consistent with the deposition of H2A.Z at these locations (Venters and Pugh, 2009; Shimada et al., 2008). One possibility is that SWR-C typically incorporates H2A.Z within a large number of nucleosomes that encompass and flank a target promoter (Figure 7). In this case, we envision that INO80 confers boundary function, removing the H2A.Z from coding region nucleosomes, reinforcing the targeted, SWR-C-dependent deposition at promoter nucleosomes. In this model, both SWR-C and INO80 may be recruited to the promoter or coding region of a target gene, or, alternatively, INO80 may function in a more general fashion, much like that proposed for the global action of histone deacetylases. Two studies have provided evidence that INO80 may be targeted to the coding regions of many genes transcribed by RNAPII (Klopf et al., 2009; Venters and Pugh, 2009), perhaps through interactions with the transcription elongation complex.

A second model is based on the fact that INO80 is associated with stalled and elongating replication forks (Papamichos-Chronakis and Peterson, 2008; Shimada et al., 2008; Vincent et al., 2008), and in this capacity INO80 controls elongation rate and fork stability. One attractive possibility is that INO80 at the replication fork may remove or replace H2A.Z that might be mislocalized during the chromatin assembly process that occurs following fork passage. In this case, H2A.Z may be deposited ectopically by fork-associated histone chaperones or deposited aberrantly by SWR-C. In either case, removal by Ino80 might then facilitate the reincorporation of H2A.Z at the proper locations by SWR-C.

INO80 and H2A.Z Acetylation

H2A.Z contains several lysine residues that are subject to reversible acetylation in all systems where it has been investigated. In *Tetrahymena*, these H2A.Z lysines are essential for cell viability (Ren and Gorovsky, 2001), whereas in budding and fission yeast the substitution of H2A.Z N-terminal lysines by arginine results in sensitivity to drugs that impact chromosome segregation but no other obvious phenotypes (Keogh et al., 2006; Kim et al., 2009). Acetylated H2A.Z is enriched at transcriptionally active promoters where H2A.Z is preferentially evicted, and it has been suggested that H2A.Z acetylation may facilitate reassembly of H2A.Z nucleosomes during gene repression (Millar et al., 2006). However, substitution alleles that remove H2A.Z lysines do not have a major impact on gene expression profiles (Millar et al., 2006). Unfortunately, commercial antibodies that recognize acetylated H2A.Z do not function in ChIP assays, so detailed analysis of the distribution and dynamics of acetylated H2A.Z has not been possible (Keogh et al., 2006; M.P.-C. and C.L.P, unpublished data).

We were surprised to find that INO80 has a large impact on the steady state levels of H2A.Z acetylation. Indeed, the analysis of bulk H2A.Z acetylation suggests that most, if not all, of the mislocalized H2A.Z is likely to be unacetylated in an *ino80* mutant. Strikingly, the genetics indicate that it is the

mislocalization of unacetylated H2A.Z that has a major impact on genome stability, not mislocalization of H2A.Z per se. The combination of mutations that disrupt the INO80 complex and the H2A.Z 4K-Q version suppresses the sensitivity of *ino80*, *arp5*, or *arp8* mutants to DNA damage and replication stress agents. In contrast, expression of the H2A.Z 4K - > R version causes an enhanced sensitivity to these same agents. These data indicate that mislocalization of unacetylated H2A.Z is an inhibitor of genome stability that must either be acetylated or be removed by INO80.

Why Is Mislocalized H2A.Z Detrimental for Genome Integrity?

The distinctive enrichment of the H2A.Z histone variant at promoter proximal nucleosomes has led to the pervasive view that H2A.Z is a key regulator of transcription that creates a more permissive environment for transcriptional activation. In yeast, loss of H2A.Z has a relatively minor effect on gene expression profiles, typically affecting only the transcriptional kinetics of a subset of inducible genes (Meneghini et al., 2003). However, our studies indicate that mislocalized H2A.Z exerts a general, repressive effect on processes that prevent genomic instability. Thus, although the promoter localization of H2A.Z provides a sensitive readout for proper deposition, perhaps the prevention of H2A.Z mislocalization by INO80 is more important than actual promoter proximal positioning. One intriguing possibility is that promoter localization places H2A.Z in a location that enhances its removal, thereby limiting its inhibitory effects on genome stability and allowing it to be used as a mechanism of transcriptional regulation.

Why does mislocalized, unacetylated H2A.Z impact DSB repair and replisome function? One possibility is that nucleosomal arrays that contain large amounts of H2A.Z assume more compact, folded states that block access of repair enzymes or destabilize stalled forks. Indeed, in vitro studies indicate that H2A.Z incorporation facilitates formation of condensed 30-nm-like fibers (Fan et al., 2002, 2004). Alternatively, perhaps H2A.Z nucleosomes are inherently more dynamic, and genome stability is impacted by the inappropriate localization of dynamic nucleosome hotspots. And finally, the acetylation state of H2A.Z may regulate interactions with protein(s) that promote or hinder genome stability. In any of these cases, the H2A.Z panacetyl mimic suppresses defects in both DNA damage repair and replication stress pathways because of loss of INO80, suggesting a common function for acetylated H2A.Z.

Elucidating the mechanisms that protect genome stability is an essential step toward understanding and fighting devastating diseases like cancer (Halazonetis et al., 2008). Our work has uncovered a chromatin-mediated pathway essential for the maintenance of genome integrity that implicates the function of the INO80 chromatin-remodeling enzyme on H2A.Z-containing chromatin. Recently, two groups provided evidence that the human INO80 complex also participates in DNA damage repair and in DNA replication, promoting genome stability (Hur et al., 2010; Wu et al., 2007). Additionally, studies in cancer patients have reported overexpression of H2A.Z in several major types of malignancies (Dunican et al., 2002; Rhodes et al., 2004; Svotelis et al., 2010; Zucchi et al., 2004). Given that the INO80 complex is highly conserved throughout evolution, both structurally and functionally (Conaway and Conaway, 2009), it would be particularly interesting to test whether the metazoan INO80 complex, similar to its yeast counterpart, regulates the localization and dynamics of the H2A.Z histone variant in higher eukaryotes.

EXPERIMENTAL PROCEDURES

Chromatin Immunoprecipitation

ChIPs were performed as described (Liu et al., 2005; Papamichos-Chronakis and Peterson, 2008) with commercially available polyclonal antibodies raised against H2A.Z (Millipore and Abcam antibodies were used for microarray analyses; Millipore and Active Motif antibodies were used for nucleosome-scanning assays). Antibody specificity was confirmed by both ChIP and western analyses (Figure S7). Mononucleosomes were prepared as described (Liu et al., 2005). The recovered DNA was subjected to quantitative real-time PCR. All ChIPs were performed at least twice and the variation between experiments was 10%–25%. Primers used in the PCR reactions are available upon request. Microarray hybridization and analysis were conducted as described (Liu et al., 2005).

Chromatin Fractionation and Protein Analysis

Chromatin fractionation was conducted as described (Liang and Stillman, 1997; Wang et al., 2009). For MNase release of nucleosome-associated proteins from the chromatin pellet, pellets were resuspended in 200 μl Lysis 1% Triton X buffer containing 1 mM $CaCl_2$ and 15 units of MNase. Samples were incubated at 37°C for 20 min and reaction was stopped by the addition of 1 mM EGTA and 1 mM EDTA. Samples were subsequently centrifuged at 14,000 rpm for 5 min at 4°C, and the supernatant was recovered for protein and DNA analysis. Equal MNase digestion was confirmed by agarose gel visualization of the released DNA.

Cell-Cycle Arrest and Flow Cytometry Analysis

Cell-cycle arrest and FACS were performed as described (Papamichos-Chronakis and Peterson, 2008).

Protein Purifications

INO80-TAP and SWR1-TAP were purified as described (Sinha et al., 2009). ATPase assay and remodeling assays were performed as described (Logie and Peterson, 1999). Recombinant yeast histones were expressed and purified from *Escherichia coli*, and octamers were reconstituted as described (Luger et al., 1999a, 1999b).

In Vitro Histone-Exchange Assay

Mononucleosomes were reconstituted by salt dialysis onto a 200 bp DNA fragment containing the 601 nucleosome-positioning sequence. Mononucleosomes were incubated with remodeling enzymes, free histone dimers, and 2 mM ATP in exchange buffer (70 mM NaCl, 10 mM Tris-HCl [pH8.0], 5 mM MgCl2, 0.1 mg/ml BSA, and 1 mM DTT at 30°C for 60 min). To reconstitute biotinylated mononucleosomes, 200 bp 601 DNA fragment was generated by PCR with biotinylated DNA primers. The biotinylated mononuclesomes were immobilized onto Dynabeads M-280 (Invitrogen). After washing to remove unbound mononucleosomes, the immobilized mononucleosomes were incubated with remodeling enzymes, free histone dimers, and 2 mM ATP in exchange buffer at room temperature for 60 min. The immobilized mononucleosomes were washed three times with exchange buffer and subjected to SDS-PAGE and western blotting.

ACCESSION NUMBERS

The Gene Expression Omnibus accession number for the microarray data reported in this paper is GSE25722.

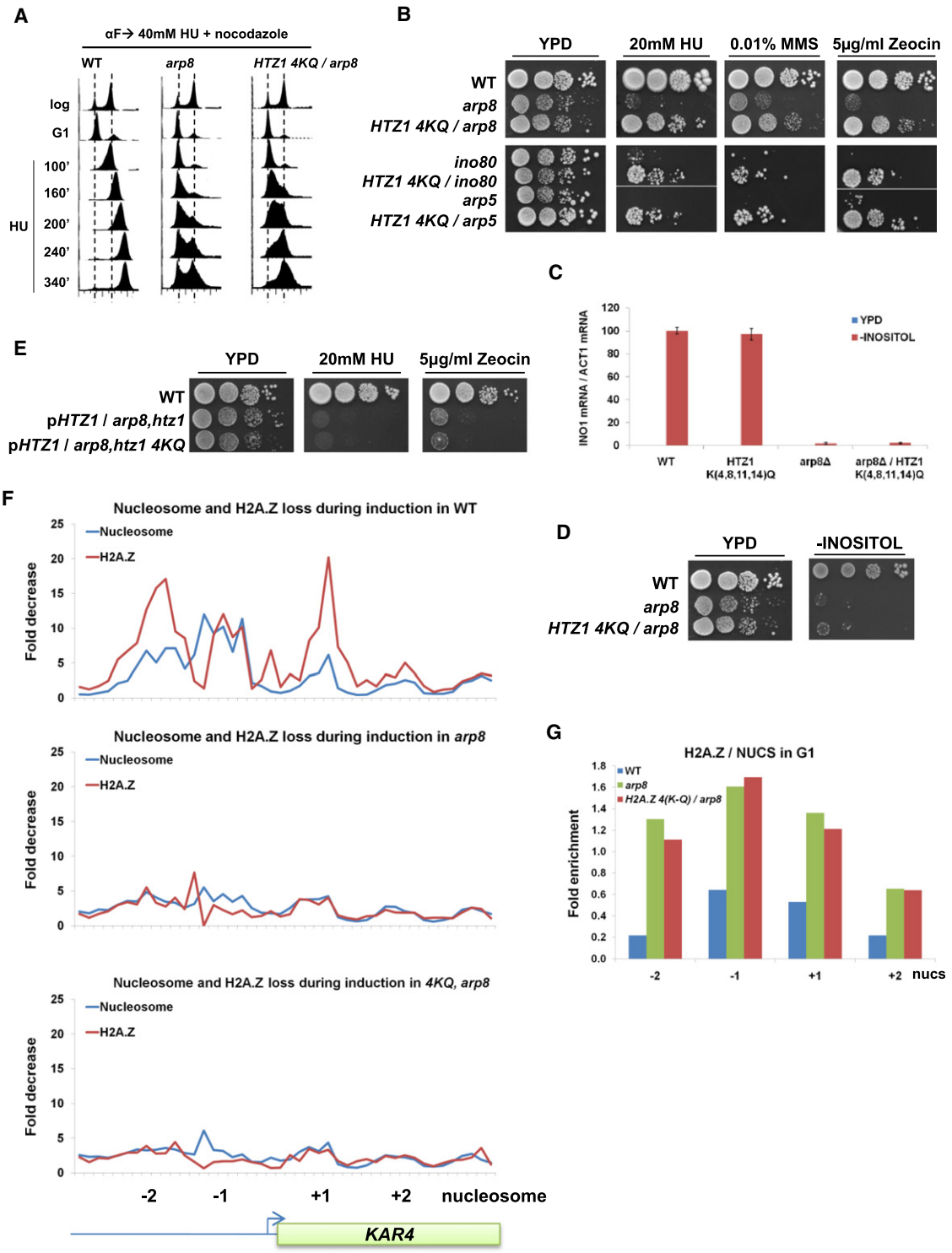

Figure 6. The Genomic Instability Phenotypes Caused by Disruption of the INO80 Complex Are Rescued by the H2A.Z-K(3,8,10,14)Q Acetylation Mimic Mutant

(A) WT, *arp8*, and *arp8* mutant cells expressing the *HTZ1-K(3,8,10,14)Q* allele (*HTZ1 4KQ,arp8*) were synchronized in G1 phase with alpha factor (αF) and subsequently released into nocodazole-containing YPD media with 40 mM HU. Cell samples were collected at the indicated times and analyzed for DNA content by flow cytometry analysis.

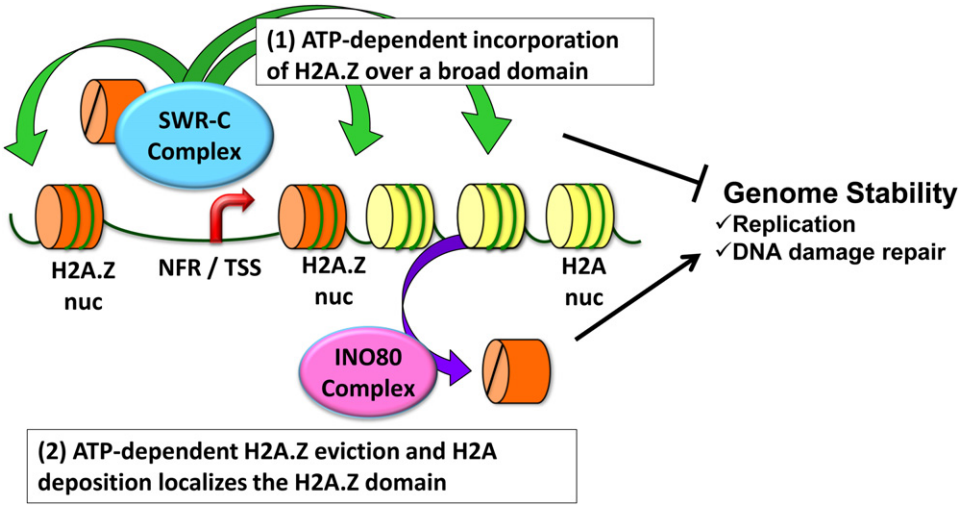

Figure 7. Proposed Model for the Role of the INO80 Chromatin-Remodeling Complex in Establishing the Proper Chromatin Localization of H2A.Z

In this model, INO80 performs a boundary function by removing H2A.Z that is deposited distal to the targeted SWR-C enzyme. See text for details.

SUPPLEMENTAL INFORMATION

Supplemental Information includes Supplemental Experimental Procedures and seven figures and can be found with this article online at doi:10.1016/j.cell.2010.12.021.

ACKNOWLEDGMENTS

This work was supported by grants from the National Institutes of Health to C.L.P. (GM54096). O.J.R. is supported in part by a Career Award in the Biomedical Sciences from the Burroughs Wellcome Fund and grants from the National Institute of General Medical Sciences and Human Frontier Science Program. M.P.-C. is supported by the Avenir Program from Inserm. We thank John Holik [University of Massachusetts Medical School (UMMS)] for assistance with the tiling array studies, Jerry Workman (Stowers Institute) for yeast histone expression vectors, John Lescyz (UMMS) for mass spectrometry analysis, Nicholas Adkins (UMMS) for the western blot with Millipore α-Htz1 sera (Figure S7), Erica Hong (Harvard Medical School) for help with Figure 7, members of the Peterson lab for helpful discussions throughout the course of this work, and Genevieve Almouzni (Curie Institute), Angela Taddei (Curie Institute), and Valerie Borde (Curie Institute)for critical reading of the manuscript.

Received: May 26, 2010
Revised: October 18, 2010
Accepted: December 15, 2010
Published: January 20, 2011

REFERENCES

Albert, I., Mavrich, T.N., Tomsho, L.P., Qi, J., Zanton, S.J., Schuster, S.C., and Pugh, B.F. (2007). Translational and rotational settings of H2A.Z nucleosomes across the Saccharomyces cerevisiae genome. Nature *446*, 572–576.

Babiarz, J.E., Halley, J.E., and Rine, J. (2006). Telomeric heterochromatin boundaries require NuA4-dependent acetylation of histone variant H2A.Z in Saccharomyces cerevisiae. Genes Dev. *20*, 700–710.

Begley, T.J., Rosenbach, A.S., Ideker, T., and Samson, L.D. (2002). Damage recovery pathways in Saccharomyces cerevisiae revealed by genomic phenotyping and interactome mapping. Mol. Cancer Res. *1*, 103–112.

Clapier, C.R., and Cairns, B.R. (2009). The biology of chromatin remodeling complexes. Annu. Rev. Biochem. *78*, 273–304.

Conaway, R.C., and Conaway, J.W. (2009). The INO80 chromatin remodeling complex in transcription, replication and repair. Trends Biochem. Sci. *34*, 71–77.

(B) WT and *arp8, ino80*, or *arp5* single mutant cells ectopically expressing from the *URA3* locus either the WT (*HTZ1*) or the *HTZ1-K(3,8,10,14)Q* (*HTZ1 4KQ,arp8*) allele were plated in 10-fold serial dilutions on YPD plates containing the indicated concentration of HU, methylmethanesulfonate (MMS) or zeocin to induce DNA replication stress, DNA damage during replication, or DNA DSBs, respectively. Pictures of the plates were taken after 2–5 days incubation at 30°C.
(C) RT-qPCR analysis of *INO1* mRNA isolated from the indicated strains grown either in the presence of inositol [yeast extract, peptone, dextrose (YPD)] or for 2 hours in synthetic media lacking inositol (−inositol). The values of *INO1* mRNA were normalized to the respective *ACT1* transcripts and normalized *INO1* transcript in WT cells grown in the absence of inositol was arbitrarily set as 100. Error bars represent variation between two separate experiments.
(D) Cells from the indicated strains were plated in 10-fold serial dilutions on YPD plates or plates containing synthetic media lacking inositol. Pictures of the plates were taken after 2–4 days incubation at 30°C.
(E) Resistance of the *HTZ1-K(3,8,10,14)Q arp8* cells to genomic instability-inducing agents is due to the *HTZ1-K(3,8,10,14)Q* locus. p*HTZ1/arp8, htz1Δ* and p*HTZ1/arp8, htz1-4KQΔ* strains were plated in 10-fold serial dilutions on YPD plates containing the indicated concentration of HU and zeocin. Pictures were taken after 2–4 days days incubation at 30°C.
(F) Nucleosome and H2A.Z loss during transcriptional induction are similar in the *HTZ1 arp8* (*arp8)* and *htz1-K(3,8,10,14)Q arp8* (*htz1-4KQ arp8*) strains. Representative graphs demonstrating nucleosome and H2A.Z loss at the *KAR4* promoter in the indicated strains. The fold decrease rates were measured as in Figure 2E. (G) Similar high enrichment of H2A.Z and H2A.Z-K(3,8,10,14)Q at the *KAR4* locus in the absence of *arp8*. Mononucleosomal-ChIP for H2A.Z was conducted in chromatin from the indicated strains arrested in G1 by alpha factor. Analysis was conducted as in Figure 2G.
See also Figure S6.

Dunican, D.S., McWilliam, P., Tighe, O., Parle-McDermott, A., and Croke, D.T. (2002). Gene expression differences between the microsatellite instability (MIN) and chromosomal instability (CIN) phenotypes in colorectal cancer revealed by high-density cDNA array hybridization. Oncogene *21*, 3253–3257.

Fan, J.Y., Gordon, F., Luger, K., Hansen, J.C., and Tremethick, D.J. (2002). The essential histone variant H2A.Z regulates the equilibrium between different chromatin conformational states. Nat. Struct. Biol. *9*, 172–176.

Fan, J.Y., Rangasamy, D., Luger, K., and Tremethick, D.J. (2004). H2A.Z alters the nucleosome surface to promote HP1alpha-mediated chromatin fiber folding. Mol. Cell *16*, 655–661.

Groth, A., Rocha, W., Verreault, A., and Almouzni, G. (2007). Chromatin challenges during DNA replication and repair. Cell *128*, 721–733.

Halazonetis, T.D., Gorgoulis, V.G., and Bartek, J. (2008). An oncogene-induced DNA damage model for cancer development. Science *319*, 1352–1355.

Hardy, S., Jacques, P.E., Gevry, N., Forest, A., Fortin, M.E., Laflamme, L., Gaudreau, L., and Robert, F. (2009). The euchromatic and heterochromatic landscapes are shaped by antagonizing effects of transcription on H2A.Z deposition. PLoS Genet. *5*, e1000687.

Hur, S.K., Park, E.J., Han, J.E., Kim, Y.A., Kim, J.D., Kang, D., and Kwon, J. (2010). Roles of human INO80 chromatin remodeling enzyme in DNA replication and chromosome segregation suppress genome instability (. Cell. Mol. Life Sci. *67*, 2283–2296.

Keogh, M.C., Mennella, T.A., Sawa, C., Berthelet, S., Krogan, N.J., Wolek, A., Podolny, V., Carpenter, L.R., Greenblatt, J.F., Baetz, K., et al. (2006). The Saccharomyces cerevisiae histone H2A variant Htz1 is acetylated by NuA4. Genes Dev. *20*, 660–665.

Kim, H.S., Vanoosthuyse, V., Fillingham, J., Roguev, A., Watt, S., Kislinger, T., Treyer, A., Carpenter, L.R., Bennett, C.S., Emili, A., et al. (2009). An acetylated form of histone H2A.Z regulates chromosome architecture in Schizosaccharomyces pombe. Nat. Struct. Mol. Biol. *16*, 1286–1293.

Klopf, E., Paskova, L., Sole, C., Mas, G., Petryshyn, A., Posas, F., Wintersberger, U., Ammerer, G., and Schuller, C. (2009). Cooperation between the INO80 complex and histone chaperones determines adaptation of stress gene transcription in the yeast Saccharomyces cerevisiae. Mol. Cell. Biol. *29*, 4994–5007.

Kobor, M.S., Venkatasubrahmanyam, S., Meneghini, M.D., Gin, J.W., Jennings, J.L., Link, A.J., Madhani, H.D., and Rine, J. (2004). A protein complex containing the conserved Swi2/Snf2-related ATPase Swr1p deposits histone variant H2A.Z into euchromatin. PLoS Biol. *2*, E131.

Krogan, N.J., Keogh, M.C., Datta, N., Sawa, C., Ryan, O.W., Ding, H., Haw, R.A., Pootoolal, J., Tong, A., Canadien, V., et al. (2003). A Snf2 family ATPase complex required for recruitment of the histone H2A variant Htz1. Mol. Cell *12*, 1565–1576.

Kurihara, L.J., Stewart, B.G., Gammie, A.E., and Rose, M.D. (1996). Kar4p, a karyogamy-specific component of the yeast pheromone response pathway. Mol. Cell. Biol. *16*, 3990–4002.

Liang, C., and Stillman, B. (1997). Persistent initiation of DNA replication and chromatin-bound MCM proteins during the cell cycle in cdc6 mutants. Genes Dev. *11*, 3375–3386.

Lin, Y.Y., Qi, Y., Lu, J.Y., Pan, X., Yuan, D.S., Zhao, Y., Bader, J.S., and Boeke, J.D. (2008). A comprehensive synthetic genetic interaction network governing yeast histone acetylation and deacetylation. Genes Dev. *22*, 2062–2074.

Liu, C.L., Kaplan, T., Kim, M., Buratowski, S., Schreiber, S.L., Friedman, N., and Rando, O.J. (2005). Single-nucleosome mapping of histone modifications in S. cerevisiae. PLoS Biol. *3*, e328.

Logie, C., and Peterson, C.L. (1999). Purification and biochemical properties of yeast SWI/SNF complex. Methods Enzymol. *304*, 726–741.

Luger, K., Rechsteiner, T.J., and Richmond, T.J. (1999a). Expression and purification of recombinant histones and nucleosome reconstitution. Methods Mol. Biol. *119*, 1–16.

Luger, K., Rechsteiner, T.J., and Richmond, T.J. (1999b). Preparation of nucleosome core particle from recombinant histones. Methods Enzymol. *304*, 3–19.

Mavrich, T.N., Jiang, C., Ioshikhes, I.P., Li, X., Venters, B.J., Zanton, S.J., Tomsho, L.P., Qi, J., Glaser, R.L., Schuster, S.C., et al. (2008). Nucleosome organization in the Drosophila genome. Nature *453*, 358–362.

Meneghini, M.D., Wu, M., and Madhani, H.D. (2003). Conserved histone variant H2A.Z protects euchromatin from the ectopic spread of silent heterochromatin. Cell *112*, 725–736.

Millar, C.B., Xu, F., Zhang, K., and Grunstein, M. (2006). Acetylation of H2AZ Lys 14 is associated with genome-wide gene activity in yeast. Genes Dev. *20*, 711–722.

Mizuguchi, G., Shen, X., Landry, J., Wu, W.H., Sen, S., and Wu, C. (2004). ATP-driven exchange of histone H2AZ variant catalyzed by SWR1 chromatin remodeling complex. Science *303*, 343–348.

Morrison, A.J., and Shen, X. (2009). Chromatin remodelling beyond transcription: the INO80 and SWR1 complexes. Nat. Rev. Mol. Cell Biol. *10*, 373–384.

Morrison, A.J., Kim, J.A., Person, M.D., Highland, J., Xiao, J., Wehr, T.S., Hensley, S., Bao, Y., Shen, J., Collins, S.R., et al. (2007). Mec1/Tel1 phosphorylation of the INO80 chromatin remodeling complex influences DNA damage checkpoint responses. Cell *130*, 499–511.

Papamichos-Chronakis, M., and Peterson, C.L. (2008). The Ino80 chromatin-remodeling enzyme regulates replisome function and stability. Nat. Struct. Mol. Biol. *15*, 338–345.

Papamichos-Chronakis, M., Krebs, J.E., and Peterson, C.L. (2006). Interplay between Ino80 and Swr1 chromatin remodeling enzymes regulates cell cycle checkpoint adaptation in response to DNA damage. Genes Dev. *20*, 2437–2449.

Peterson, C.L., and Cote, J. (2004). Cellular machineries for chromosomal DNA repair. Genes Dev. *18*, 602–616.

Raisner, R.M., Hartley, P.D., Meneghini, M.D., Bao, M.Z., Liu, C.L., Schreiber, S.L., Rando, O.J., and Madhani, H.D. (2005). Histone variant H2A.Z marks the 5′ ends of both active and inactive genes in euchromatin. Cell *123*, 233–248.

Ren, Q., and Gorovsky, M.A. (2001). Histone H2A.Z acetylation modulates an essential charge patch. Mol. Cell *7*, 1329–1335.

Rhodes, D.R., Yu, J., Shanker, K., Deshpande, N., Varambally, R., Ghosh, D., Barrette, T., Pandey, A., and Chinnaiyan, A.M. (2004). Large-scale meta-analysis of cancer microarray data identifies common transcriptional profiles of neoplastic transformation and progression. Proc. Natl. Acad. Sci. USA *101*, 9309–9314.

Ruhl, D.D., Jin, J., Cai, Y., Swanson, S., Florens, L., Washburn, M.P., Conaway, R.C., Conaway, J.W., and Chrivia, J.C. (2006). Purification of a human SRCAP complex that remodels chromatin by incorporating the histone variant H2A.Z into nucleosomes. Biochemistry *45*, 5671–5677.

Shen, X., Mizuguchi, G., Hamiche, A., and Wu, C. (2000). A chromatin remodelling complex involved in transcription and DNA processing. Nature *406*, 541–544.

Shen, X., Ranallo, R., Choi, E., and Wu, C. (2003). Involvement of actin-related proteins in ATP-dependent chromatin remodeling. Mol. Cell *12*, 147–155.

Shimada, K., Oma, Y., Schleker, T., Kugou, K., Ohta, K., Harata, M., and Gasser, S.M. (2008). Ino80 chromatin remodeling complex promotes recovery of stalled replication forks. Curr. Biol. *18*, 566–575.

Sinha, M., Watanabe, S., Johnson, A., Moazed, D., and Peterson, C.L. (2009). Recombinational repair within heterochromatin requires ATP-dependent chromatin remodeling. Cell *138*, 1109–1121.

Svotelis, A., Gevry, N., Grondin, G., and Gaudreau, L. (2010). H2A.Z overexpression promotes cellular proliferation of breast cancer cells. Cell Cycle *9*, 364–370.

Talbert, P.B., and Henikoff, S. (2010). Histone variants–ancient wrap artists of the epigenome. Nat. Rev. Mol. Cell Biol. *11*, 264–275.

Venters, B.J., and Pugh, B.F. (2009). A canonical promoter organization of the transcription machinery and its regulators in the Saccharomyces genome. Genome Res. *19*, 360–371.

Vincent, J.A., Kwong, T.J., and Tsukiyama, T. (2008). ATP-dependent chromatin remodeling shapes the DNA replication landscape. Nat. Struct. Mol. Biol. *15*, 477–484.

Wang, A.Y., Schulze, J.M., Skordalakes, E., Gin, J.W., Berger, J.M., Rine, J., and Kobor, M.S. (2009). Asf1-like structure of the conserved Yaf9 YEATS domain and role in H2A.Z deposition and acetylation. Proc. Natl. Acad. Sci. USA *106*, 21573–21578.

Wu, W.H., Alami, S., Luk, E., Wu, C.H., Sen, S., Mizuguchi, G., Wei, D., and Wu, C. (2005). Swc2 is a widely conserved H2AZ-binding module essential for ATP-dependent histone exchange. Nat. Struct. Mol. Biol. *12*, 1064–1071.

Wu, S., Shi, Y., Mulligan, P., Gay, F., Landry, J., Liu, H., Lu, J., Qi, H.H., Wang, W., Nickoloff, J.A., et al. (2007). A YY1-INO80 complex regulates genomic stability through homologous recombination-based repair. Nat. Struct. Mol. Biol. *14*, 1165–1172.

Yuan, G.C., Liu, Y.J., Dion, M.F., Slack, M.D., Wu, L.F., Altschuler, S.J., and Rando, O.J. (2005). Genome-scale identification of nucleosome positions in S. cerevisiae. Science *309*, 626–630.

Zhang, H., Roberts, D.N., and Cairns, B.R. (2005). Genome-wide dynamics of Htz1, a histone H2A variant that poises repressed/basal promoters for activation through histone loss. Cell *123*, 219–231.

Zucchi, I., Mento, E., Kuznetsov, V.A., Scotti, M., Valsecchi, V., Simionati, B., Vicinanza, E., Valle, G., Pilotti, S., Reinbold, R., et al. (2004). Gene expression profiles of epithelial cells microscopically isolated from a breast-invasive ductal carcinoma and a nodal metastasis. Proc. Natl. Acad. Sci. USA *101*, 18147–18152.